UNIVERSITY OF CAGLIARI

Faculty of Mathematical, Physical and Natural Sciences

Degree Course in Physics

Time response of a GSO crystal

Supervisor:
Prof. Biagio Saitta

Candidate:
Giacomo Caria

Academic Year 2011-2012

Acknowledgements

Foremost, I would like to express my sincere gratitude to my supervisor Prof. Biagio Saitta, for his patience, motivation, expertise and wide knowledge. His guidance deeply helped me in all the time of experimental work and writing of this thesis.

I am also grateful to Prof. Alessandro Cardini, for his useful help for both experimental and theoretical matters.

Last but not least, I would like to thank my family for the essential support provided throughout all these years and for letting me free to choose my personal path.

Contents

List of Figures

List of Tables

Introduction

The aim of this work is a measurement of the decay time of a crystal of the inorganic scintillator GSO, Cerium-doped Gadolinium orthosilicate, Gd_2SiO_5:Ce, in the context of a project which studies the feasibility of an active, electron polarized detector to be used with neutrino (and anti-neutrino) beams [1],[2].

One of the interesting characteristics of the GSO in fact is that, being a paramagnetic crystal, it can be temporarily polarized, albeit only for a small electron fraction; the polarization changes the cross-sections and thus provides a new degree of freedom in the understanding of the properties of the interacting particles. The properties of GSO have been extensively studied since its discovery in 1983 by Takagi and Fukazawa [3]; the value of the decay time has been measured and found to depend on the Ce concentration [5], [6], therefore it is of interest to perform an independent measurement on the actual crystal used to study the magnetic properties.

The technique used for this work is known as time-correlated single photon counting (TCSPC) and it is based on the theoretical consideration that the function describing the rate of photons emitted per second by a scintillator must have, apart for a normalization factor, the same shape of the probability distribution function (PDF) of the emitting process. As a consequence, recording a large number of elapsed times between the scintillation events and the emission of single and randomly independent photons, it is possible to construct an experimental PDF histogram, and its fit with a theoretical model will provide the decay process characteristic time.

One of the features of the experimental setup is that it has to record single photons which are casually uncorrelated with one another. This result is achieved by placing a detector at a proper distance from the GSO crystal, so that at most one photon will reach, at a very slow rate, the device for each scintillation event. In general as single-photon sensitive detector a Photomultiplier Tube (PMT), a Micro Channel Plate (MCP) or a Single Photon Avalanche Diode (SPAD) can be used. Also, to reduce light intensity, a neutral density filter can be inserted between the PMT and the GSO crys-

tal, as used in other measurements. In our experimental setup a PMT was used, in some instances with the photocathode partially masked to reduce the sensitive area.

Among the possible methods to measure the excitation time, for practical reasons, a PMT attached to the GSO was used.

Chapter 1

Methods and materials

1.1 Scintillation mechanism in inorganic crystals

Energy release in a material, which will consequentially emit light, can occur in different ways. Incandescence is the process where thermal motion is transformed into electromagnetic radiation, while we refer to luminescence for all the other processes which do not involve heat. For instance, energy may be released in the material by a mechanical action as in triboluminescence, or supplied by chemical reaction as in chemiluminescence, while when excitation is caused by incident electromagnetic radiation we have photoluminescence. More in detail, we define fluorescence as photoluminescence or scintillation which presents a fast decay time, approximately 10^{-9} to 10^{-7} sec, while longer times are the main characteristics of phosphorescence, 10^{-6} to 10^{3} sec.

Scintillation, i.e. light emission yielded by ionization radiations of charged particle which excite the material, differs for the following materials: inorganic crystals, organic crystals, noble gases and liquids, plastic scintillators. We will examine further how light emission occurs in inorganic crystals [4], since the topic of this thesis is the GSO scintillator. In these substances scintillation depends strongly on the crystal band structure. In fact, ionization causes the transfer of electrons from the valence band into the conduction band, and consequentially vacancies (known as holes) are left in the valence band, for many purposes can be thought as physical particles with positive charge +e which are free to move in the valence band.

Although this mechanism creates a pair of electron and hole that are not coupled, in other cases, i.e. the formation of an exciton, the pair can be tightly bound and move as a single particle in the crystal, with the electron excited to an energy level just below the conduction band, in that region

known as forbidden band. Impurities play a fundamental role in the scintillation process, since they provide a site for the recombination of electron-hole pairs. In fact, this can happen when a hole free to move in the valence band comes close to an atom impurity, also called activator site. The latter will be ionized by a migrating free hole or a hole from an exciton pair , as one of its electrons escapes from the fundamental state. As a consequence electrons can be captured in the activator excited states and decay in the activator ground state, with the emission of scintillation light. Impurities centers are strongly efficient since the dopant atom is left in its original state so that each center may partecipate in many recombination.

When the electron is placed in an activator excited states with forbidden transitions to the ground state, known as metastable states, it requires an additional energy to move into another excited state where it is finally free to decay, or may decay spontaneously, but the latter options is highly improbable . This mechanism needs a long time that is, as previously stated, the main property of phosphorescence. Another reason for slow light emission is the formation of traps, which may be defined as sites with energies in the forbidden band, where only one type of charge carrier is accepted, avoiding therefore the possibility of recombination. Such centers hold the electron or the hole and release it after a certain characteristic time.

Our energy source is a γ-ray emitter, therefore we will not have many inelastic collisions with atomic electrons, a typical property of charged particles. Instead, photons interact with matter by:

1. Photoelectric effect
2. Compton scattering
3. Pair production

The interaction cross section through each of these mechanisms is energy dependent, photoelectric effect and Compton scattering being dominant at low and medium energy and pair production at high energy with an onset at 1.02 MeV, the mass energy of an electron-positron pair at rest.

1.2 TCSPC method

The easiest method for measuring the time decay of the scintillation process would be to directly fit a pulse shape, i.e. the number of photons emitted per unit time as a function of time, recorded as electronic signal, by a theoretical function. Nevertheless, for the intrinsic limits of electronic devices, we can not rely on this procedure. The solution to this problem is the technique

called time-correlated single photon counting, described by Bollinger and Thomas [7].

We define a probability distribution function (PDF) $p(t, t_{start})$ such that the probability of emitting a single scintillation photon in the time interval $t, t + dt$ after the interaction of a γ-photon with a crystal scintillator at the time t_{start} is equal to $p(t, t_{start}) \cdot dt$. This distribution is equal to the scintillation pulse shape, except for a normalization factor, therefore our goal of measuring the decay time of the GSO crystal may be achieved recording a large number of single scintillation photons and constructing empirically the PDF.

In more detail, we are interested in the time elapsed between the absorption of the incident radiation by the crystal (which defines $t = 0$) and the emission of these single scintillation photons, whose distribution is indeed probabilistically determined. It is important to stress that the photons registered by the stop detector have to be not only single but also statistically independent. Consider the case where several photons produced by the same scintillation event reach the stop detector. It will be triggered by the first photon in arrival order, which will be also the only one providing an arrival time for calculating the requested time difference with the start time.

It is easy to see how this affects the statistical foundation of the TCSPC method. Recording only the first photons, we have an over-representation of early arrival times, an effect called pile-up, since all the other later times can not be collected and are in fact discarded, so that the true randomness of essential value for this technique is lost.

In order to avoid biasing the data which will fill the histogram and in turn permit to draw the pulse shape, the experimental setup must be designed in such a way that even the possibility of detecting one single photon per scintillation event is low. As a consequence, this ensures that probabilities for the stop detector to detect two or more photons are absolutely negligible.

1.3 Experimental setup

As start and stop detectors for the TCSPC measurements two photomultiplier tubes HAMAMATSU H6533 have been used. This device, sensitive between 300 to 650 nm, with a wavelength of maximum response of 420 nm close to the GSO emission wavelength, has been chosen mainly for its fast response, which includes a rise time and a transit time spread (TTS) of 0.7 ns and 0.16 ns respectively.

All measurements were performed at room temperature. The power supply is a programmable CAEN model N471. PMTs were operated at different

voltages, 2000 V for the start detector and 2250 V for the stop detector.

The GSO crystal, with dimensions 2x2x10 mm^3, is excited by a ^{60}Co radioactive source which is a γ-ray emitter.

One of the PMTs, which we will refer to as start detector, is attached to the GSO crystal and coupled optically to it using a optical grease in order to optimize the light collection. These conditions permit the start detector to collect a large amount of light, so that early emitted photons in the scintillation event hit surely the detector, providing the start time for the TCSPC method.

From the side of the crystal opposite to the one attached to the *start detector*, light can reach the second PMT, which we will refer to as *stop detector*. As emphasized in the theoretical section, the rate at which single photons arrive at the stop detector must be exceptionally low, so that the probability for receiving two or more photons emitted in the same scintillation event is absolutely negligible, hence ensuring that the fundamental condition for the TCSPC technique is satisfied. As a consequence the stop PMT detector has been placed at a variable distance d from the crystal and in one case its aperture has been properly adjusted with a pinhole to reduce further the light intensity.

In order to avoid false-stop signals, which are time interval measurements of stop pulses and start signals not causally correlated, mainly due to dark noise, both start an stop PMTs signals were fed into a low threshold CAEN N224 discriminator which accepts only events above the thresholds set at 10.5 mV and 2.5 mV respectively, and forms NIM pulses (400ns wide).

Discriminator signals were read out by the oscilloscope LeCroy 104MXi, which calculated time difference between the 50% amplitudes and created a histogram for all measured start-stop differences, yielding the experimental pulse shape.

The logic of the data acquisition is schematically represented in fig. 1.1.

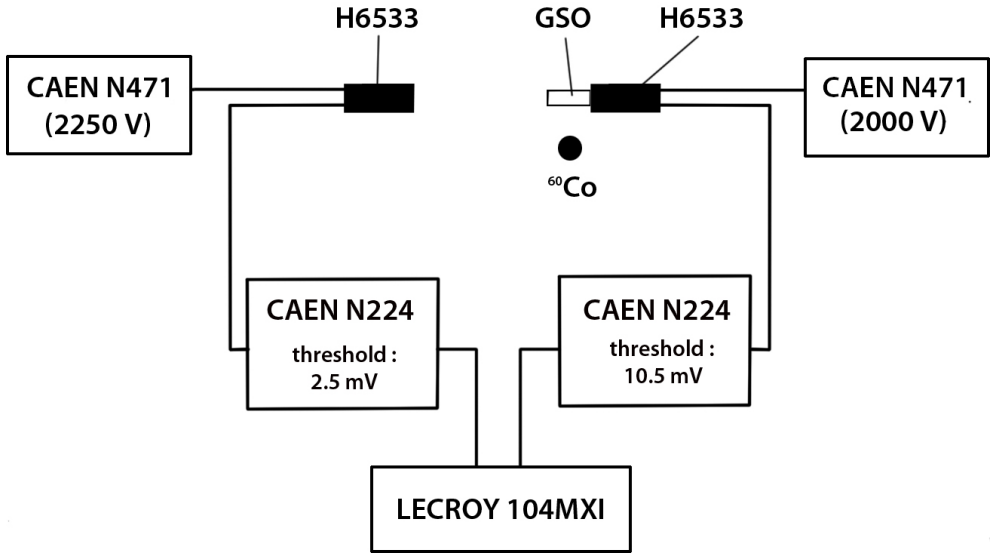

Figure 1.1: Experimental setup used for the measurement of the decay time of GSO

Chapter 2

Results

2.1 Detectors timing performance

Values of several tens of nanoseconds for the so-called "fast" component and several hundreds of nanoseconds for the "slow" component are reported in literature for GSO scintillator.

To ascertain the capability of our system to measure values of that order as well as to estimate its intrinsic time resolution, two additional set of measurements were carried out in the setup:

1. Time difference when both photomultipliers are in contact with the scintillating GSO crystal and

2. a complete set of measurements at various distances, with the GSO replaced by a small cylinder of plastic scintillator EJ-200 of size similar to that of the inorganic crystal.

For the first set of measurements a slightly modified setup was used, to allow both photomultipliers to be in contact with the scintillator (either GSO or EJ-200) and optically coupled to it. Also the surface of the photocathode not in contact with the scintillator was protected by a 2-mm thick lead shield to avoid photons from the Co60 source to reach directly the active surface.

The time difference between the "start-detector" and the "stop-detector" for the two cases is shown in figures 2.2 and 2.1.

In both cases the distribution is centered at slightly negative values, indicating that the PMT used as "stop-detector" has a response faster than the PMT used as "start-detector".

It is possible to observe that for both materials the time distributions is best fitted with a sum of gaussian functions. From a physics point of view

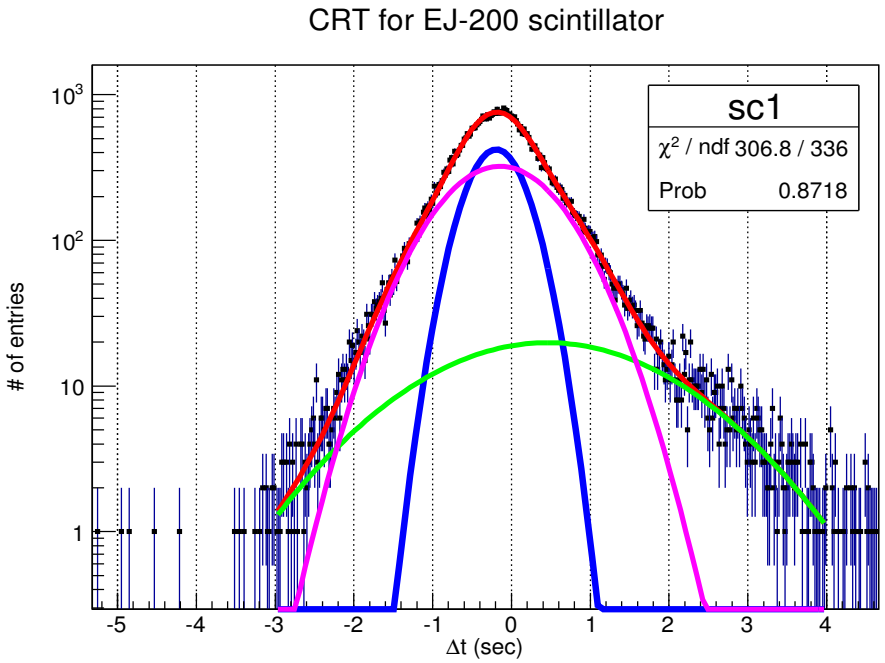

Figure 2.1: Coincidence resolution time for EJ-200 scintillator

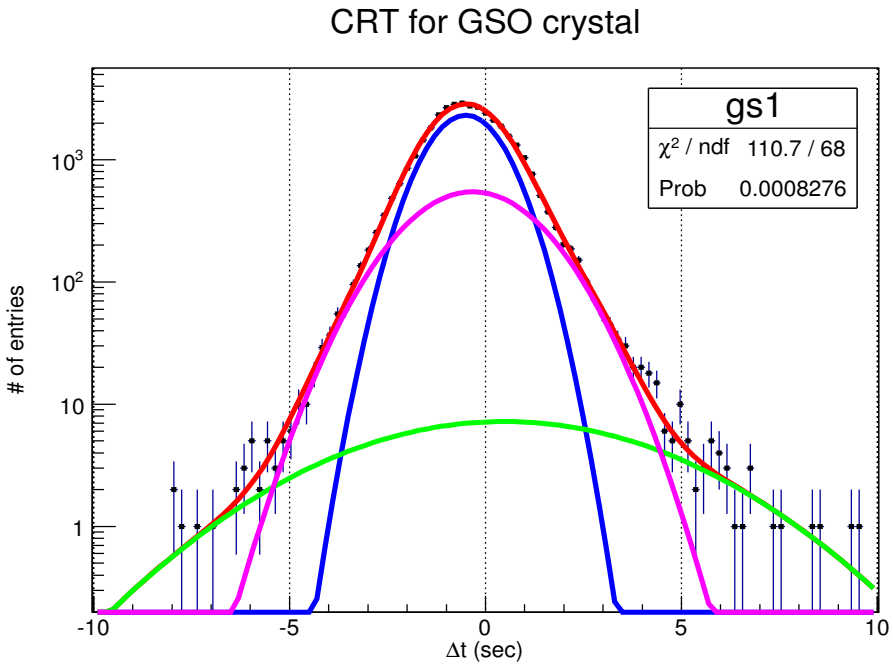

Figure 2.2: Coincidence resolution time for GSO crystal

this is explained with intrinsic differences between the two PMT detectors, and also as an effect of a different voltage they were operated at.

The different FWHM reflect the characteristic time properties of the two scintillating materials.

For the GSO crystal, the coincidence resolving time (CRT) is 2.1 ns FWHM, corresponding to a single detector timing resolution of 1.5 ns FWHM, while for the EJ-200 we obtain, respectively, 0.8 ns and 0.6 ns. These values refer to the blue gaussian curve in both figures.

A time resolution of 1.5 ns for GSO and less than 0.6 ns for EJ-200, seems to be adequate for our purposes.

2.2 Test setup using fast plastic scintillator

A set of preliminary measurements has been taken with the fast plastic scintillator EJ-200 instead of the GSO crystal, while the experimental apparatus described in the previous section remains unchanged. This new material has a decay time, 2.1 ns [9], sensibly shorter than the one we expect for the GSO, but their wavelength of maximum emission is approximately the same at around 430 nm. The goal of these measurements is to test whether the TCSPC setup is properly working, and this is done analyzing quantitatively the data obtained using a material with well-known time characteristics. The distance between the start detector, coupled optically to the plastic scintillator, and the stop detector assumes the values 1 cm, 6 cm, 16 cm and 68 cm. Recorded time difference distributions are shown respectively in the figures 2.3, 2.4, 2.5 and 2.6.

These time distributions have been analyzed with the software package ROOT [8], which allows, among many other features, to fit histograms with pre-defined or user-defined functions. A single exponential appears to describe well the data at 1cm and 68cm, while the data at 6cm and 16cm seems to require a more complex function. As previously described, light yield is composed by two contributes, the fast and the slow component. Therefore, it is natural to model the decay with a function that represents both, i.e. a two-component exponential the form:

$$N = A\exp(-t/\tau_{slow}) + B\exp(-t/\tau_{fast}) \tag{2.1}$$

where τ_{slow} and τ_{fast} are the decay constants, A and B magnitudes that vary from material to material, although the fast component usually dominates. For a better representation, histogram fittings are plotted with with a logarithmic y-axis in figures 2.7, 2.8, 2.9 and 2.10.

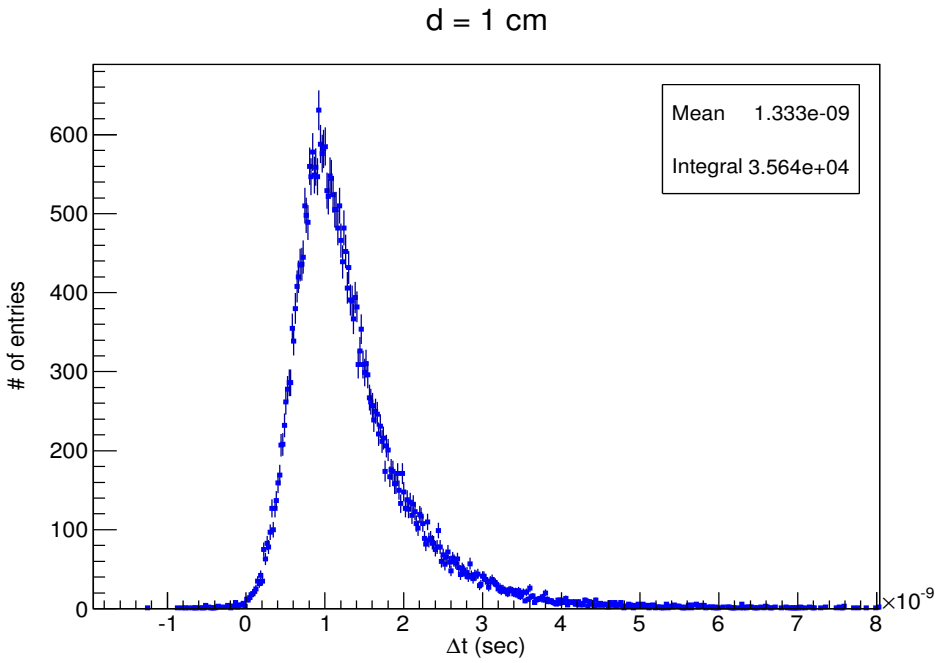

Figure 2.3: Δt distribution of EJ-200 scintillator for d = 1 cm

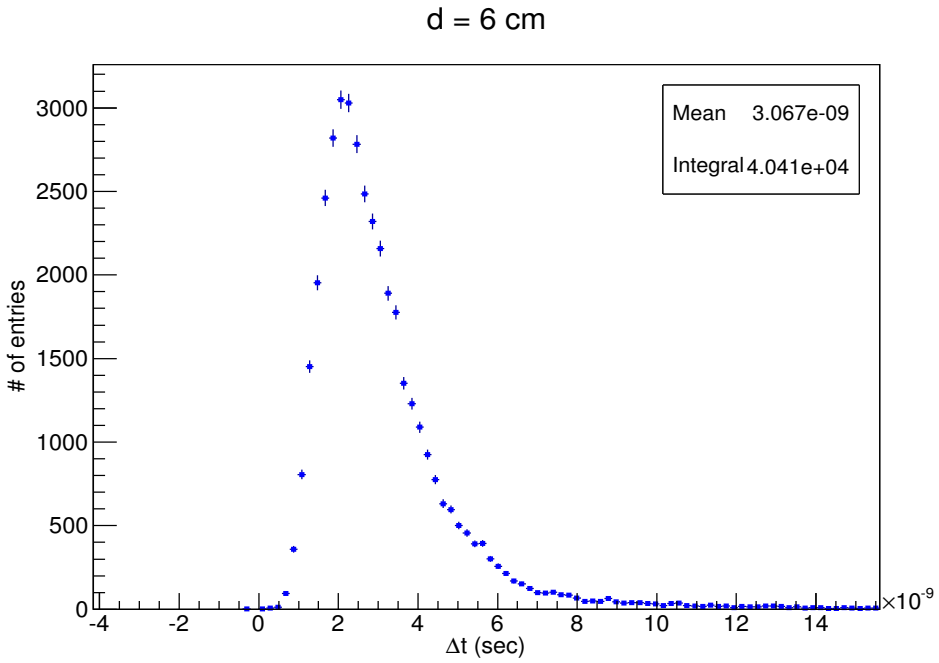

Figure 2.4: Δt distribution of EJ-200 scintillator for d = 6 cm

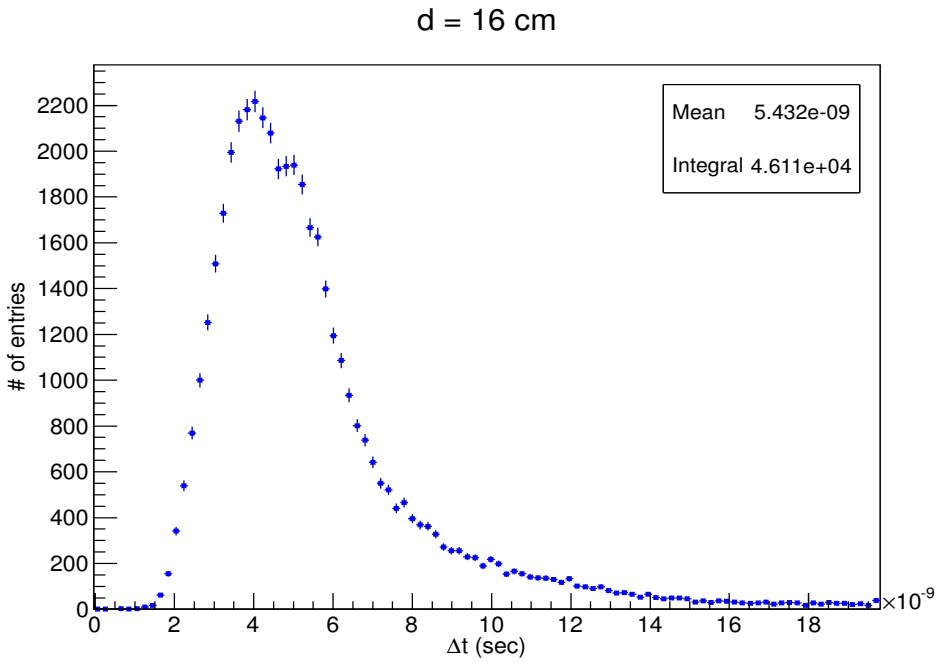

Figure 2.5: Δt distribution of EJ-200 scintillator for d = 16 cm

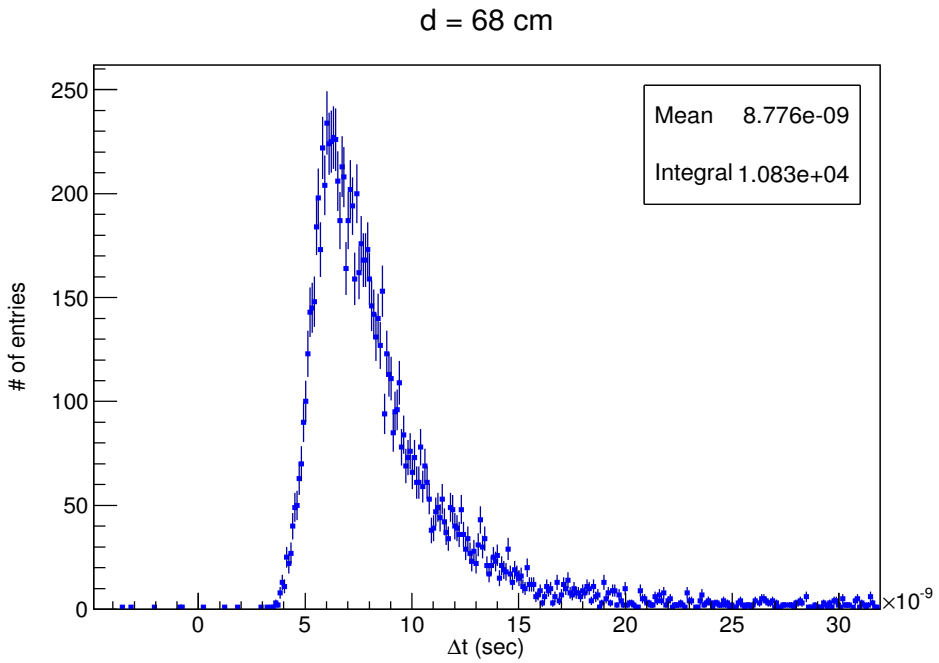

Figure 2.6: Δt distribution of EJ-200 scintillator for d = 68 cm

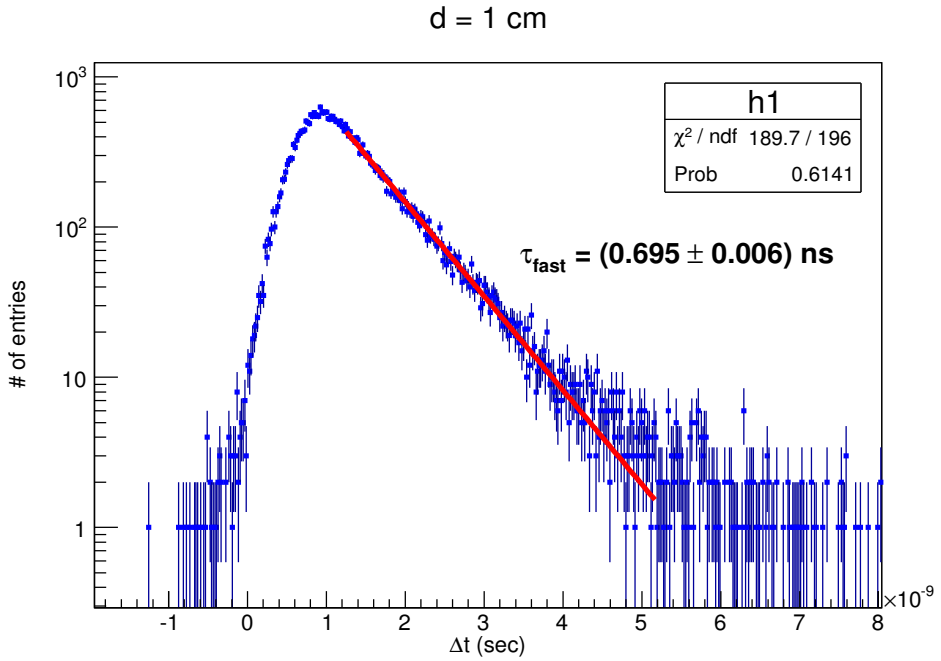

Figure 2.7: Exponential fit to data for EJ-200 scintillator and d = 1 cm

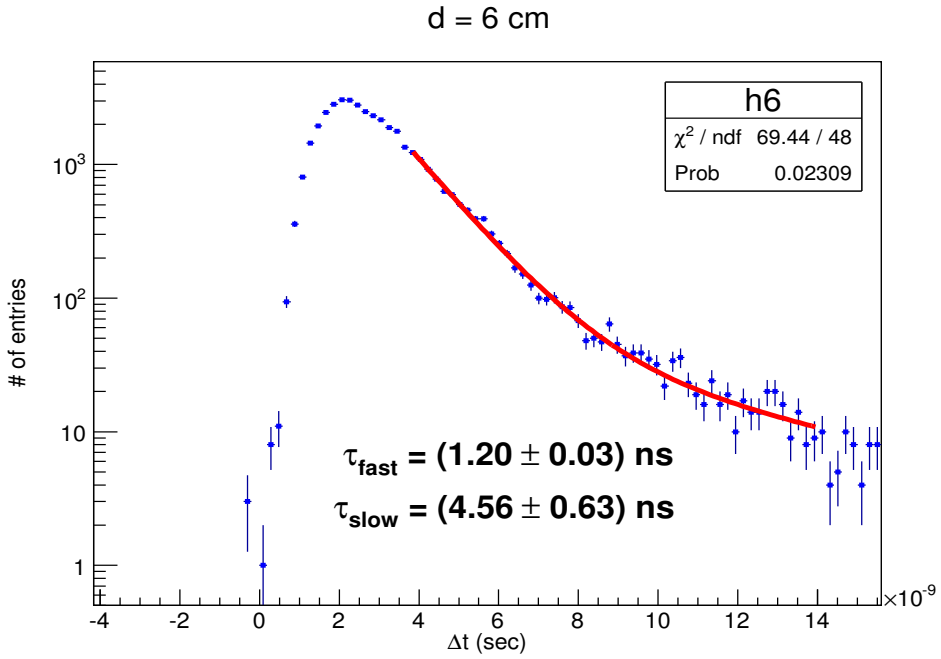

Figure 2.8: Exponentials sum fit to data for EJ-200 scintillator and d = 6 cm

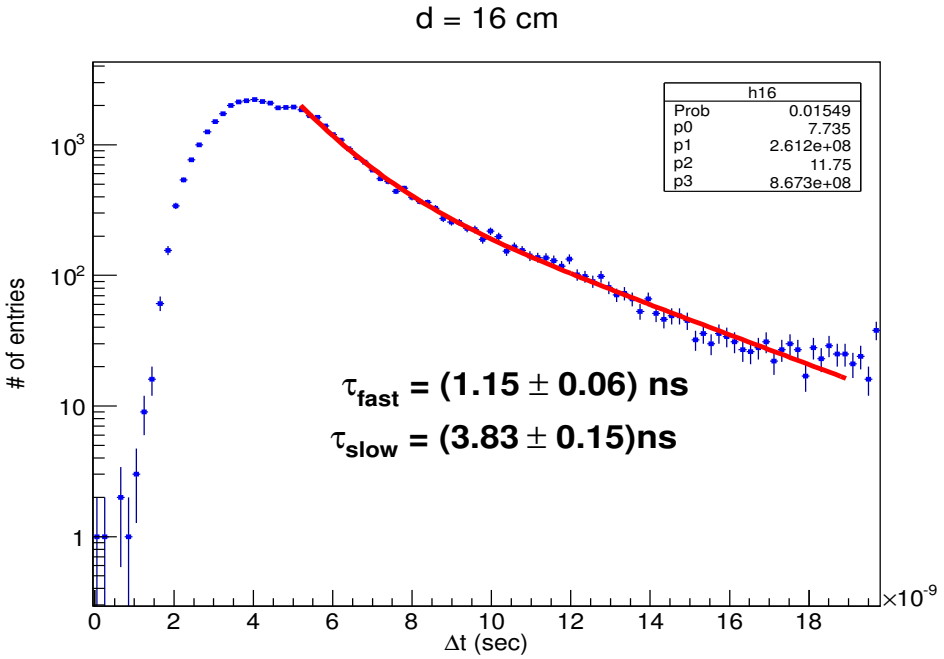

Figure 2.9: Exponentials sum fit to data for EJ-200 scintillator and d = 16 cm

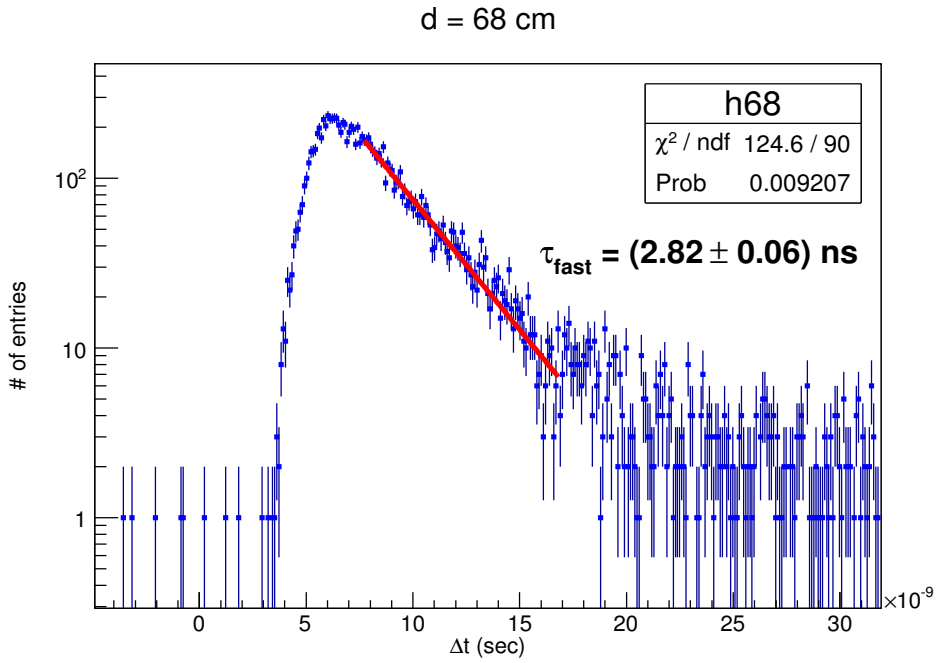

Figure 2.10: Exponential fit to data for EJ-200 scintillator and d = 68 cm

distance (cm)	τ_{fast} (ns)	τ_{slow} (ns)
1	0.695 ± 0.006	
6	1.20 ± 0.03	4.56 ± 0.63
16	1.15 ± 0.06	3.83 ± 0.15
68	2.82 ± 0.06	

Table 2.1: Results of the fit for EJ-200 scintillator

Since we chose to use the TCSPC method, the most important results we should discuss are those that are close to the single-photon condition. Hence, the histogram we may assume approximate the probability distribution, i.e the pulse shape, with our best precision for the fast plastic scintillator has been obtained with d = 68 cm. It is shown in figure 2.10.

The value obtained for the fast component, 2.8 ns, is sufficiently close to the value provided by the manufacturers, i.e. 2.1 ns. The presence of a slow component was not expected; however since is of order of few nanoseconds does not affect the characteristics of this type of scintillator.

In conclusion we have verified it can effectively sample the probability distribution and is therefore appropriate for the next main measurements of GSO crystal decay times.

Numerical values for fast components obtained fitting the data are summarized in table 2.1.

2.3 Measurement of GSO decay time

Measurements have been repeated for different distances between the start and stop detectors, namely 1 cm (fig. 2.11), 6 cm (fig. 2.12), 16 cm (fig. 2.13), 68 cm (fig. 2.14), and 16 cm with a pinhole (fig. 2.15) in order to study quantitatively how time difference distributions change when probabilities for the single-photon condition increase.

When plotted in a logarithmic scale, these histograms clearly show a double component behavior, which demonstrates the presence of the two luminescence processes: the fast luminescence and the slow phosphorescence. As a consequence, the function implemented in the software ROOT for the fit is the same as in the formula 2.1. The two exponentials sum fittings to data are shown, in order of increasing distance between detectors, in figures 2.16, 2.17, 2.18, 2.19 and 2.20.

The time distributions at different distances are plotted together in fig. 2.21 and 2.22, in order to compare them qualitatively.

The resulting parameter values for each measurement are summarized in

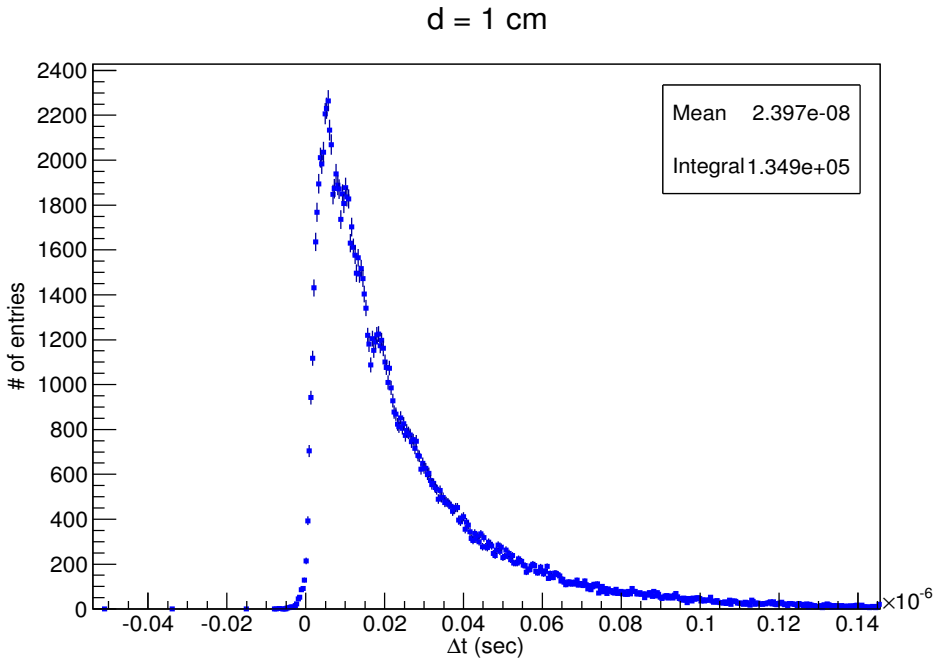

Figure 2.11: Δt distribution of GSO crystal for d = 1 cm

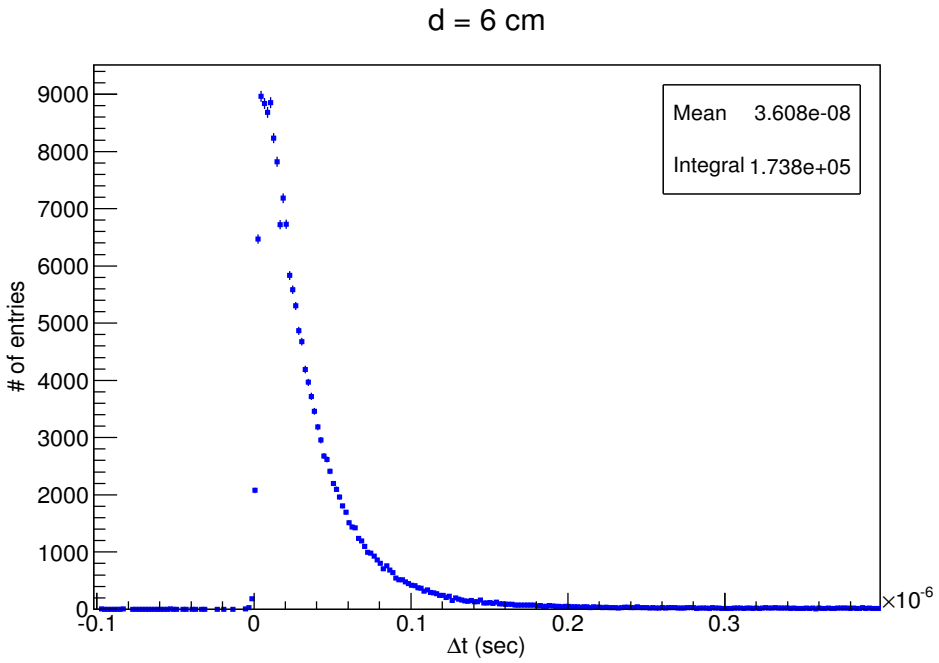

Figure 2.12: Δt distribution of GSO crystal for d = 6 cm

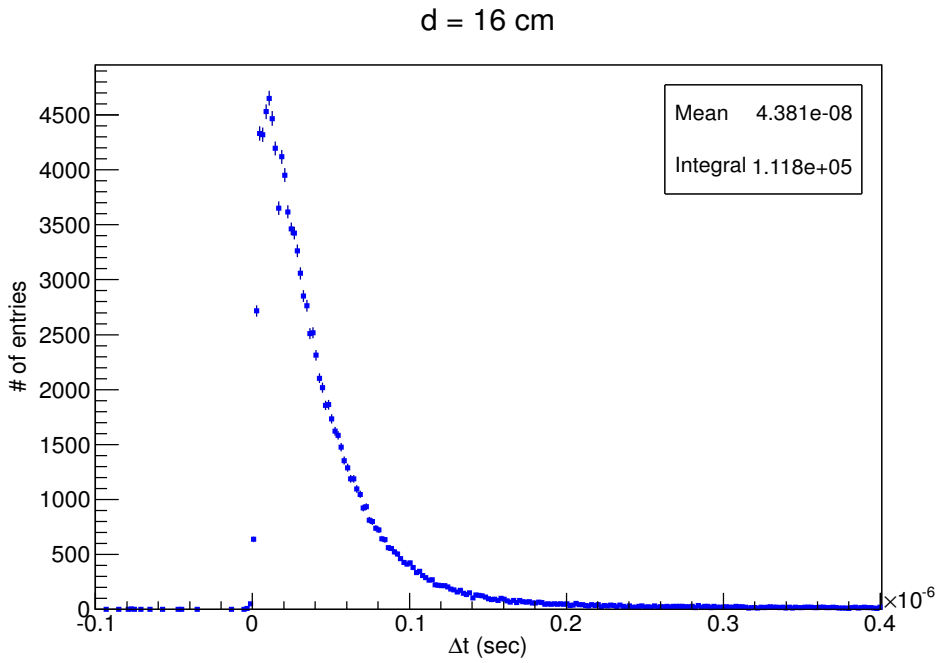

Figure 2.13: Δt distribution of GSO crystal for d = 16 cm

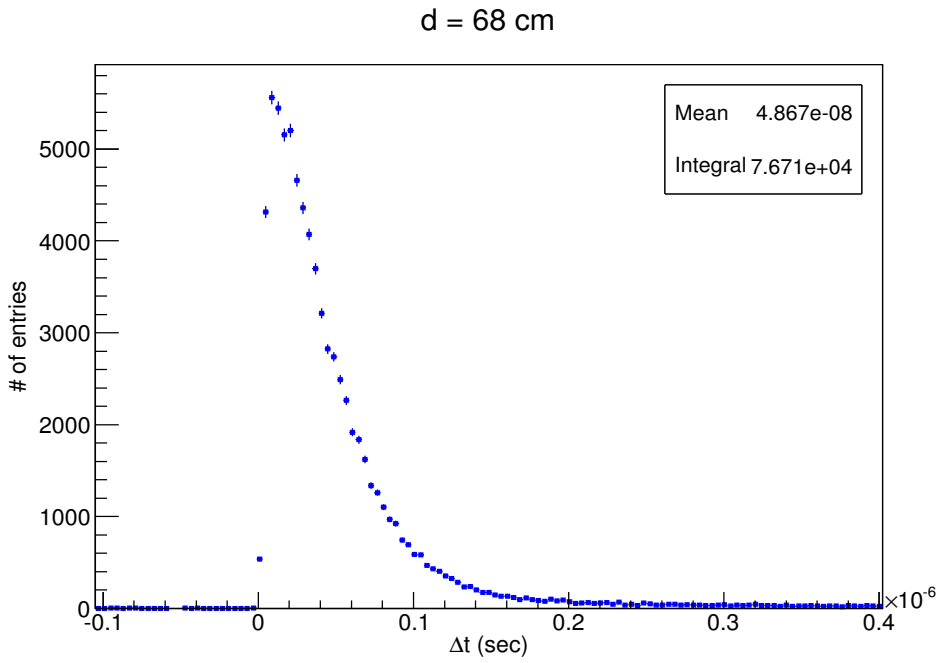

Figure 2.14: Δt distribution of GSO crystal for d = 68 cm

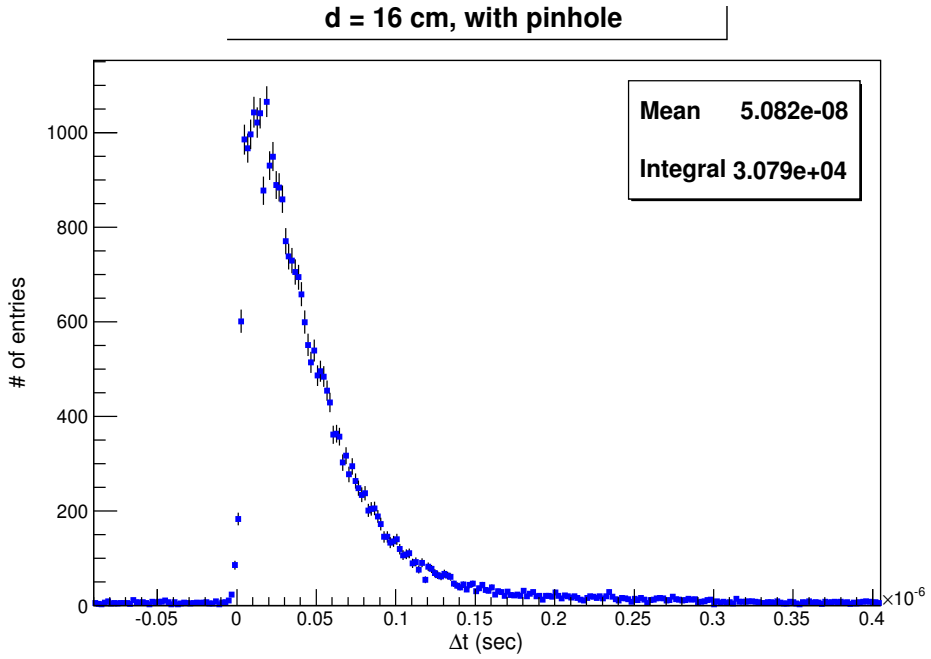

Figure 2.15: Δt distribution of GSO crystal for d = 16 cm with pinhole

table 2.2.

2.4 Conclusions

Using the TCSPC method we obtained, for the setup at 16 cm with pinhole, a value of (33.72 $\pm$ 0.58) ns and (486.5 $\pm$ 34.5) ns respectively for fast and slow components, consistent with other measurements in literature [5], but different from the value of 56 ns and 600 ns quoted for instance in [10], presumably owing the different Ce concentration in the crystal. However, as far as the fast component is observed, the values at 16 cm, 68 cm and 16 cm

distance (cm)	τ_{fast} (ns)	τ_{slow} (ns)
1	12.55 ± 0.70	31.11 ± 0.88
6	27.91 ± 0.12	221.7 ± 5.7
16	30.96 ± 0.31	234.3 ± 7.05
68	31.35 ± 0.31	374.5 ± 8.5
16, with pinhole	33.72 ± 0.58	486.5 ± 34.5

Table 2.2: Results of the fit for GSO crystal

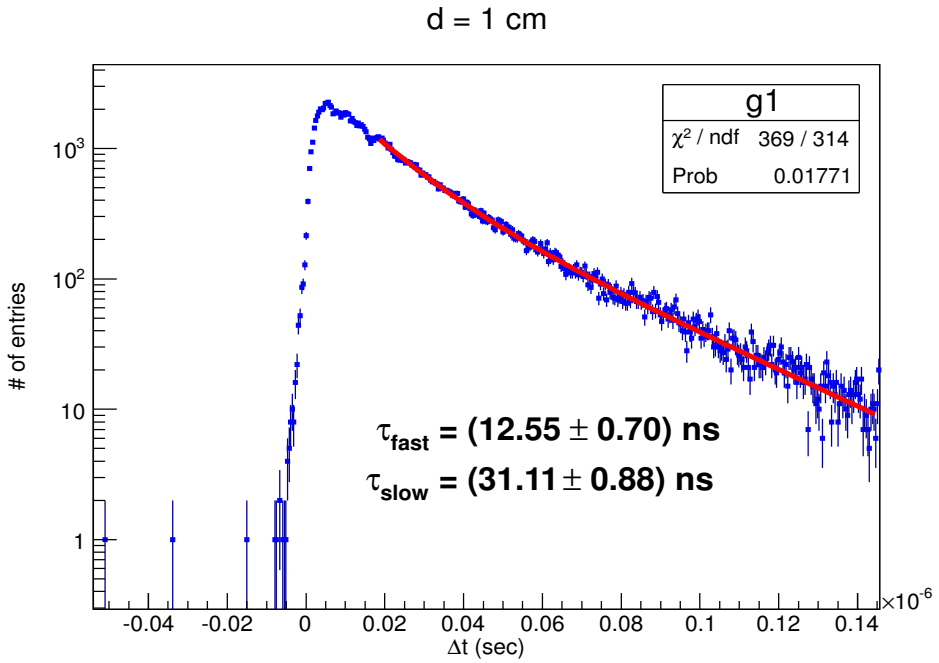

Figure 2.16: Exponential fit to data for GSO crystal for d = 1 cm

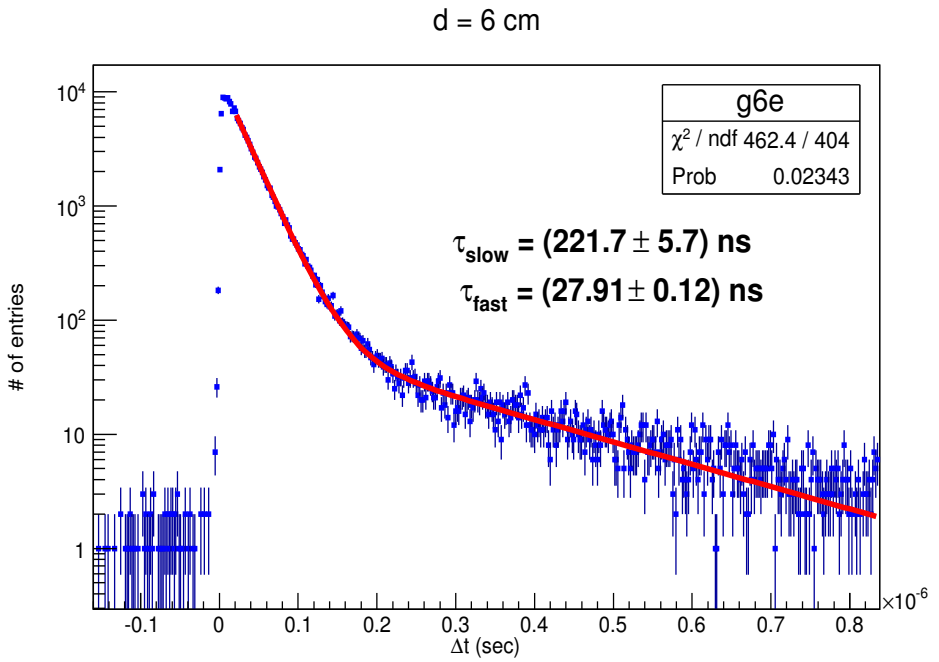

Figure 2.17: Exponentials sum fit to data for GSO crystal and d = 6 cm

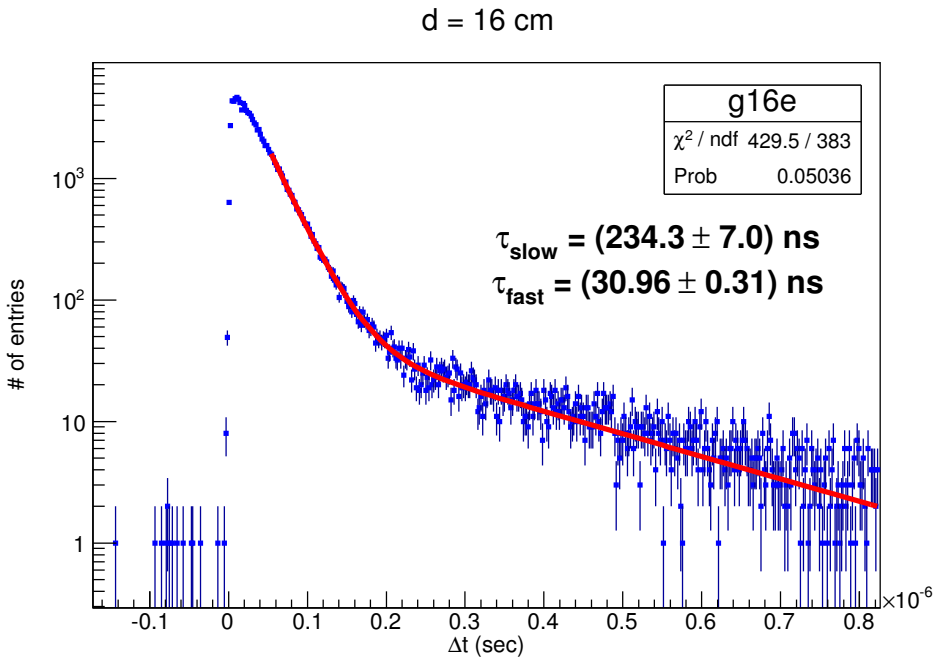

Figure 2.18: Exponentials sum fit to data for GSO crystal and d = 16 cm

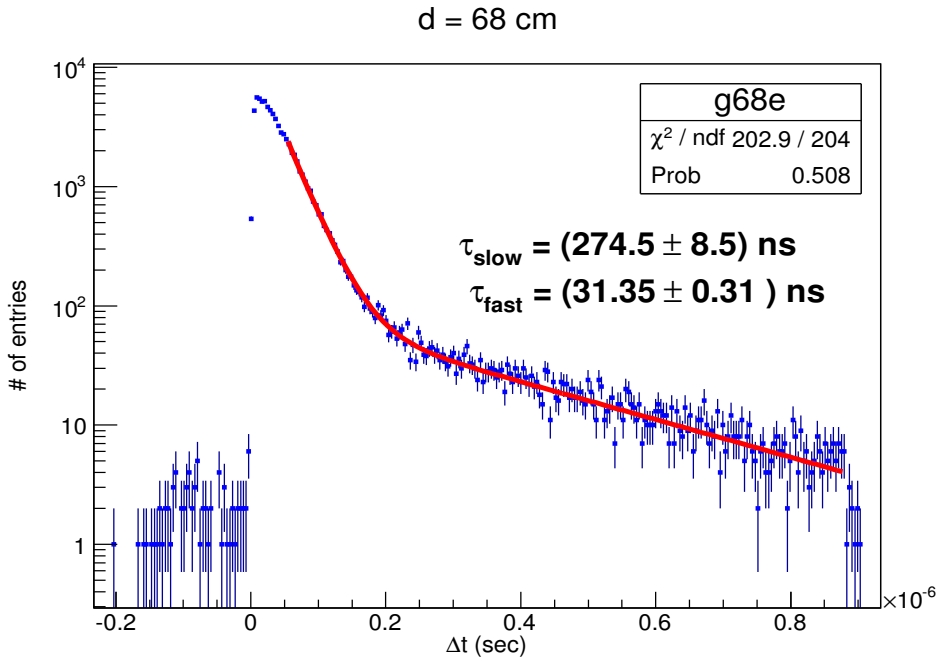

Figure 2.19: Exponentials sum fit to data for GSO crystal and d = 68 cm

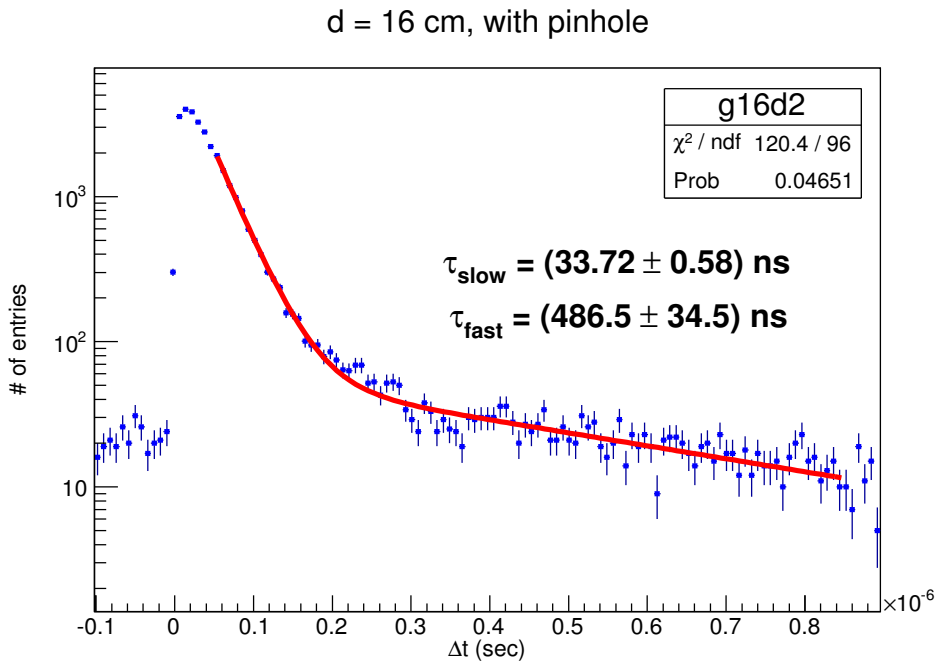

Figure 2.20: Exponentials sum fit to data for GSO crystal and d = 16, with pinhole

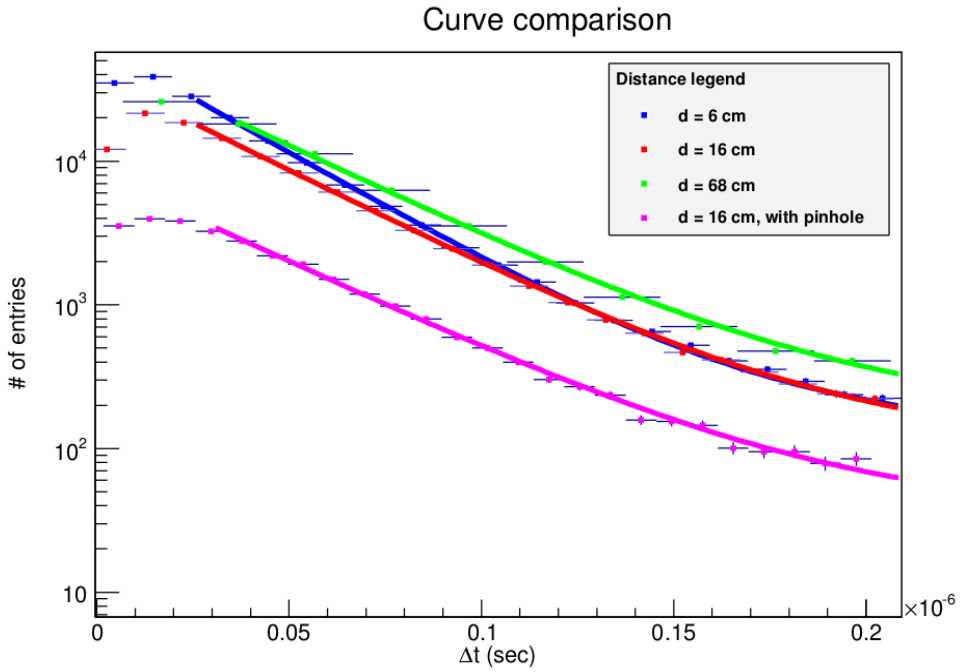

Figure 2.21: Comparison of time distributions at different distances for small Δt

with pinhole are consistent among each other, indicating that the condition of single-photon is probably reached.

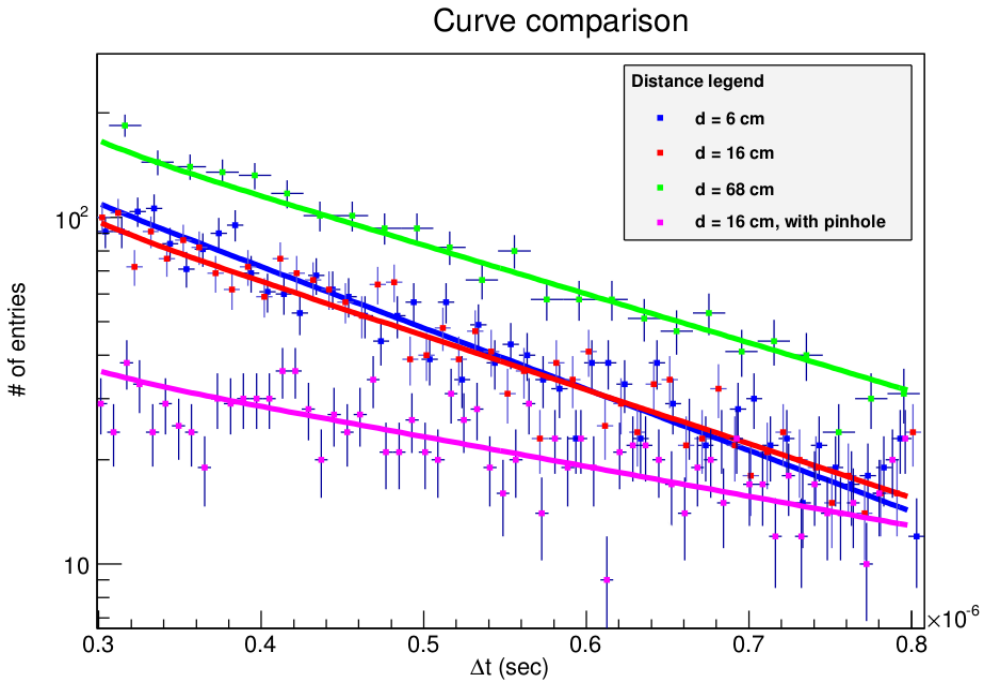

Figure 2.22: Comparison of time distributions at different distances for large Δt

Bibliography

[1] M. P. Mocci, "Studio per la realizzazione di un bersaglio attivo polarizzato magneticamente", Degree Course in Physics Thesis, University of Cagliari, 2010

[2] C. Vacca, "Fattibilita' di un esperimento per la diffusione di neutrini su elettroni polarizzati", Degree Course in Physics Thesis, University of Cagliari, 2011

[3] K. Takagi and T. Fukazawa, Appl. Phys. Lett., vol 42, no. 1, p.43, 1983

[4] W. R. Leo, "Techniques for Nuclear and Particle Physics Experiments", Springer-Verlag, Berlin Heidelberg, 1987

[5] M. Tanaka et al., "Applications of cerium-doped gadolinium silicate Gd_2SiO_5:Ce scintillator to calorimeters in high-radiation environment", *Nucl. Instr. Meth. A*, vol.404, Issue 2-3, p.283-294, 1997

[6] C. L. Melcher, J. S. Schweitzer, T. Utsu, and S. Akiyama, "Scintillation properties of GSO", *IEEE Trans. Nucl. Sci.* 37, p. 161-164, 1990

[7] L. M. Bollinger, G. E. Thomas, "Measurement of the Time Dependence of Scintillation Intensity by a Delayed-Coincidence Method", *Rev. Sci. Instr.*, vol.32, no.9, p. 1044-1050, 1961

[8] ROOT, A Data Analysis Framework, http://root.cern.ch/drupal/

[9] EJ-200 Plastic Scintillator, G-tech Corp, http://www.ggg-tech.co.jp/maker/eljen/ej-200.html

[10] R. Y. Zhu, C. L. Woody, "Inorganic scintillators", *Phys. Lett. B*, vol.667, Issue 1-5, p.286-8, 2008